Ultra-Wide-Band SAW Sensors Based on Hyperbolically Frequency Modulated Signals

Victor Plessky
GVR Trade SA
Gorgier, Switzerland
Email: victor.plessky@gvrtrade.com

Aleksey Shimko, You Jen Cho
Tai-Saw Technology Co. Ltd.
Taiwan
Email: aleksey.shimko@mail.taisaw.com,
larrycho@mail.taisaw.com

***Abstract*— A SAW (Surface Acoustic Wave) sensor including grooved-grating chirp reflectors is designed, manufactured and measured/probed on wafer. The device includes two wide-band SAW interdigital transducers (IDTs) on a YZ-cut $LiNbO_3$ substrate, operating in the frequency range of 2000MHz-2500MHz (B=500MHz), situated in parallel acoustic tracks having two dispersive reflectors operating at the same frequencies. The reflector period increases linearly with distance from the IDTs and, correspondingly, the frequency of the impulse response of the reflectors is *hyperbolically* dependent on time. The duration of the impulse response is 1000ns, so that the signal base is B*T= 500. In remote measurements, such a sensor transforms interrogation signals received from the reader in its specific way and the reflected signals can be compressed such that the processing gain is greater than 20dB compared to other parasitic reflections. In contrast to classic Linear Frequency Modulated (LFM) signals, for the proposed signal, the compression process remains invariant with respect to the thermal expansion of the sensor, which significantly simplifies the "reading" algorithms. For the measurement of temperature, the device uses two offset reflectors, with the delay between the reflection peaks being dependent on temperature. At the moment of writing this paper, the different designs of the device were probed on wafer. Compressed signals are obtained with an expected duration of about 2 ns. We plan to package the sample devices and subsequently measure them remotely using a "reader" for measuring the S11(f) on the defined frequency grid.**

Keywords – SAW sensors; hyperbolic frequency modulation; signal compression; reflecting grating; processing gain.

I. INTRODUCTION

There are a few reasons why using Ultra-Wide-Band (UWB) signals in passive, remotely-controlled, sensors and SAW-tags can be interesting [1]. Such a sensor including chirp Interdigital Transducer (IDT) or chirp reflector, reflects interrogation signals sent by the "reader" thereby significantly transforming it. Knowing how the sensor is coding the signals allows to decipher the code (for signal compression) using the "matched to signal" filtering [2]. Such a procedure results in the processing gain of B*T times because the signal of duration T is compressed into a short pulse of duration ~ 1/B. In SAW devices, we have typical delays comparable to a few microseconds. Therefore, if we can use short compressed pulses, we can read simultaneously numerous sensors by the same reader, distinguishing them by delays of the peaks. Finally, the processing gain allows increasing the reading distance, or higher accuracy of measurements, or reducing the size of a sensor.

While using LFM chirps [3], or "orthogonal frequency coding" [4], the unknown change in temperature of the sensor results in an unknown extension or compression of the impulse response of the sensor. Consequently, the reader must find the matched filter to a signal which is not exactly known, which creates additional complications to the reader algorithms. It was recently proposed [5] to use the "Hyperbolically Frequency Modulated" (HFM) signals in SAW sensors for which the period, and not frequency, of the signal linearly varies with time. The advantage of such signals is that the extension or compression of the signal is equivalent to a small shift of it in time. Therefore, for "matched to signal" compression the reader can always use the same algorithm, independent of the sensor temperature.

In this paper, the following aspects are discussed. In Section II, design of the devices along with some key parameters are presented. Experimental results of manufacturing and measurements of the devices made in frames of Swiss-Lithuanian research project [7], along with prospective application in temperature sensing after post signal processing of the measured HFM signals, is presented in Section III. The paper is concluded by presenting the advantages of using these devices for remote temperature sensing with future work in Section IV.

II. DEVICE DESIGN

The device is designed to operate at 2000-2500MHz (B=500MHz) frequency range with dispersive reflectors providing chirp reflected signal 1000ns (T=1μs) long, with the product B*T equal to 500. The device includes two parallel connected IDTs (9 fingers in each), and 2 reflectors, with either a uniform or weighted aperture, as shown in Figure 1.

Figure 1. Sensor with aperture-weighted reflectors.

 ISBN: 978-1-61208-621-7

The following numbers and dimensions were used in the design: SAW velocity inside the IDTs V_T= 3290 m/s for YZ-LN with about 70nm thick Al electrodes, the pitch in the IDTs p_T =0.73μm. For the shallow grooved reflectors on YZ-LN, the equivalent SAW velocity V_G = 3488 m/s with pitches at the beginning and at the end of reflectors p_0= 0.6976μm and p_N= 0.872μm respectively and total length of the reflectors L= 1744μm. Therefore, the number of grooves in each reflector grating is N_G= 2231. The initial delay between the IDTs and close-in reflector in different sensors were designed to be 500ns, 550 ns and 600ns, and the off-set between reflectors was always the same – equal to 500ns. The initial delay can be reduced (discussed in Section IV).

Metal (***Al***) thickness of electrodes was close to 72 nm, metallization coefficient was 0.5 on the mask, but looked higher on the wafer. The targeted nominal depth of grooves was h= 15 - 40 nm; this has not been measured yet.

III. PROBE RESULTS AND SIGNAL PROCESSING

A. Probes on the wafer

The manufactured devices were probed on wafer. We had a few wafers with evidently different quality of devices and the depth of etched grooves in reflectors seems not to be very uniform. S11(f) of the devices were measured using a Network Analyzer (NWA) from 1500-3100MHz (B=1600MHz) with a uniform grid of step 0.2MHz (8001 frequency points), providing visible delay of 5 μs.

On the Smith chart, shown in Figure 2, one can see a small loop due to impedance of the IDT in the capacitive zone, in the bottom-right quadrant of the chart. It can be matched with a series inductance of 5.5 nH reasonably close to the center of the Smith chart, with real part of admittance Re(adm) ~ 1/50 1/Ω as shown in Figure 3.

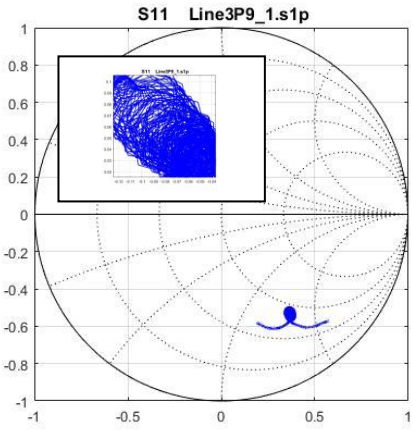

Figure 2. S11 on the Smith's chart, as measured. The insert shows the part of the curve corresponding to the reflections.

The reflected waves from the gratings arrive to the IDTs with phases fast varying with frequency and appearing as chaotic oscillations on the Smith chart as seen in the insert of Figure 2 and on the real and imaginary part of admittance, shown in Figure 3. It is also noted that the reflections are much stronger at high frequencies, close to 2.5 GHz, which run a shorter distance and hence, their propagation loss is about 6 dB lower than that of lower frequency (2.0 GHz) components. The device under test (P9) had uniform aperture and the SAW with shorter wavelength are also more strongly reflected.

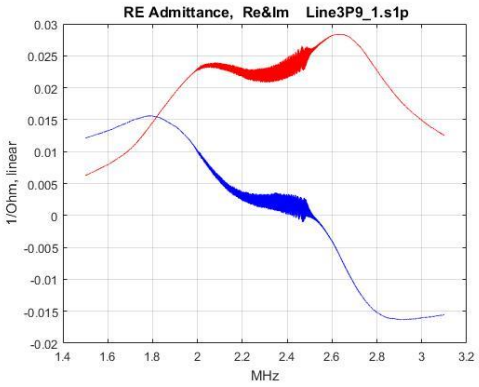

Figure 3. ReAdm(red) and ImAdm(blue).

B. Signal processing

After deleting the slowly varying part of S11, corresponding to the signal reflection from the IDT itself, we can see only the remaining contribution of the signals arriving from the reflectors, as seen in Figure 4.

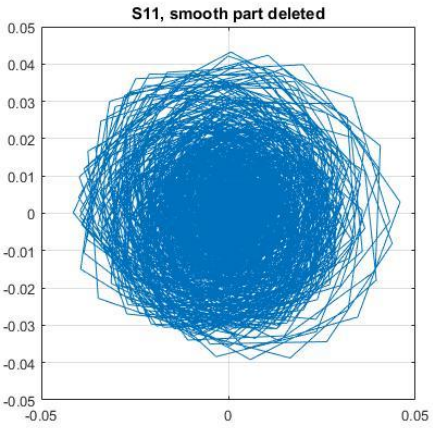

Figure 4. Fast rotating part of S11(f) – reflections from the chirp reflectors.

From Figure 4, we can estimate that the reflected signals have the level below $20*\log_{10}(0.04)$ = - 28 dB or so, at all frequencies of the reflector. The main part of the signals have losses close to -34dB.

Transforming the response from Figure 4 to the time domain, we can see the reflected pulses (impulse response of the device), as depicted in Figure 5. As expected, the reflections from the first reflector begin at a delay of 500ns and continue until 1000ns, overlapping with identical reflections from the second reflector beginning at t=1.0 μs.

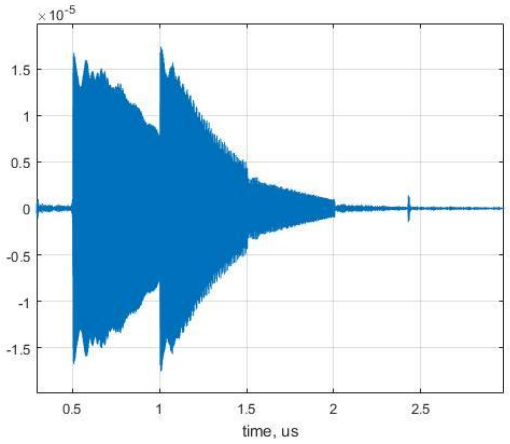

Figure 5. Reflections in time domain.

Between t= 1.0 μs and t=1.5μs both signals overlap creating beating due to the frequency change in the chirp signals, as seen in Figure 6. In order to make all periods of the signal visible, we used a so-called "zero-padding" technique, extending the frequency range to 40 GHz by filling the missing S11(f) points (outside of the actual measured frequency range) with zeros. The strong amplitude of the beats confirms that the reflected signals coming from the same distance from two reflectors have about equal amplitude, as expected.

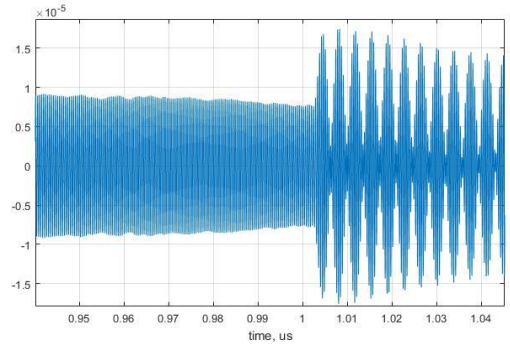

Figure 6. Overlapping of the chirp signals.

Calculating the periods of the reflected signals between the time delays 0.5μs – 1.0μs (where they do not overlap) we can see in Figure 7 that the period of this chirp signal is a linear function of time. To compress the signals, we used an ideal theoretical signal inverted in time and generated according the formulas [5]:

$$\theta_2 = -2\pi\frac{T}{B}\left(f_0^2 - \frac{B^2}{4}\right)\log\left(1 - \frac{Bt}{(f_0+B/2)T}\right) \qquad (1)$$

$$A_2 = \exp(i\theta_2) \qquad (2)$$

where T=1 μs is the duration of the signal, B=500MHz - its frequency band, f_0=2250 MHz – center frequency, and t – is current time.

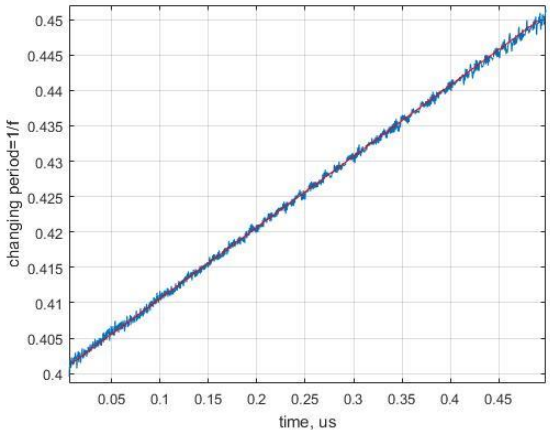

Figure 7. Periods in the signal linearly depend on time; red streight line is drawn for comparison.

This theoretical unit amplitude signal was convolved with the device response in the time domain, shown in Figure 8. The compressed pulses show -3dB duration of about 2 ns, as expected, and their amplitude is of the order of -10.5 dB (first blue peak in Figure 8), which corresponds to about 20dB of the processing gain. The brown peaks in Figure 8 correspond to the following numeric experiment. We have increased the duration of the used theoretical pulse T => 1.01 T, that is by 1%, and decreased its frequency band correspondingly (B/1.01). This would correspond to a +120°C change in temperature of "matched to signal" YZ-LiNbO3 based physical filter (if used). The experiment shows that the compression remains practically unchanged, only the compressed pulses are shifted. But the distance between the pulses is unchanged.

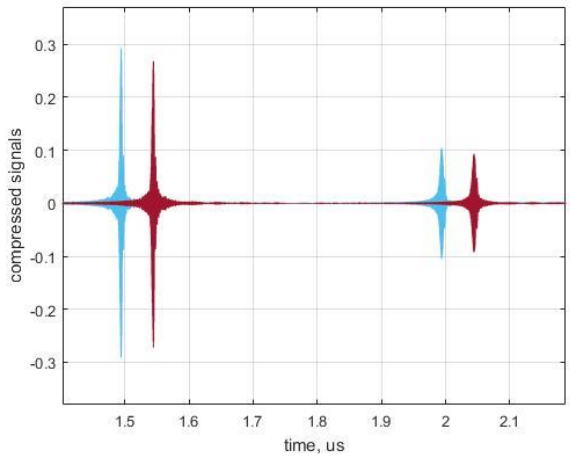

Figure 8. Compressed pulses (blue);the theoretical pulse used for colvolution extended by 1% (brownline).

Figure 9 illustrates compressed pulses for 6 probed devices. The devices consist of two sets of three designs with different initial delays. Reasonable reproducibility of results has been obtained.

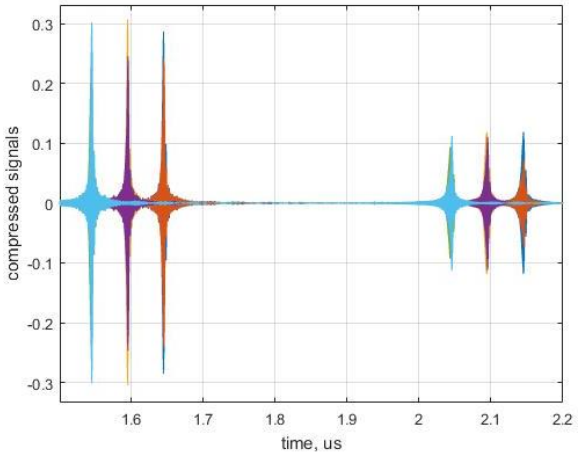

Figure 9. 6 sensors, 12 peaks.

At this scale, the compressed peaks with the same delay completely overlap.

IV. DISCUSSION AND CONCLUSIONS

The numeric experiment, illustrated by Figure 8, shows that for compression of the UWB pulses we do not need to care much about exact inversion in the time of the measured pulse. Moreover, that would be impossible without additional experimental devices, because in the present samples the reflected pulses do overlap. The compression is invariant for small changes of the reference signal as it results in a simultaneous shift of the two compressed peaks. However, the distance between said peaks remains unchanged. On the other hand, if there was a significant change in temperature of the measured sensor itself, the compression process will remain invariant, but the distance between compressed peaks is temperature dependent. Namely, this allows measurement of temperature by accurate measurement of the said time delay between the compressed peaks. The described procedure makes multiple trials of matched to signal filter parameters and, in this way, essentially simplifies reader software and accelerates extraction of the measured physical value (in this case, temperature).

Figure 9 allows us to estimate the number of sensors that can be interrogated simultaneously by one reader. The identification of the individual sensor can be done by the position of the compressed peak pairs. The distance between the reader and the sensors is of the order of a few meters and can introduce the uncertainty of the initial delay of around 10 ns. A change in temperature of 100°C introduces a variation of the 2nd peak position of the order of 20ns. Therefore, we must allocate a time slot about 30 ns long for each 2nd peak. Otherwise, the peak from a "cold" sensor might be confused with the peak of "hot" sensor separated at larger distance. In this design, we have about 500ns for all "2nd" peaks, which means that we can have 500/30 ~16 sensors interrogated simultaneously. Potentially, we could increase the off-set between the reflectors to about 1 μs, and thus, increase the possible number of interrogated sensors to about 30. On contrary, the initial delay of 500ns, serves no purpose since the compressed pulse appears after the end of the impulse response of the 1st reflector, that is after 1 μs delay in our case. Therefore, the empty space between the IDTs and the 1st reflector can be significantly reduced. The above estimations show that the maximal number of sensors interrogated by one reader is also dependent on the expected operation temperature range of the sensor system.

A. *Futher work*

After packaging a sufficient number of sensors, we plan to measure them remotely using the interrogation device ("the reader") developed earlier by T. Ostertag, RSSI GmbH, Germany [6]. The reader device measures distantly the reflected sensor signals S11(f) in a predetermined set of frequency points. According to our previous experience [1], the expected precision of the measurements must be better than 0.1°C. We plan direct experiments by varying sensor temperature. The software being developed now will fully profit from the above discussed invariance of the compression pulse procedure with respect to the sensor temperature.

Our other goal is the accurate measurement of power levels (instant and average) of the electromagnetic radiation of the reader in different measurement regimes and comparisons with existing UWB regulations.

ACKNOWLEDGMENT

This work was done within the frame of the Swiss-Lithuanian Eurostars Project No. E!10640 UWB_SENS and was co-funded by the State Secretariat for Education, Research and Innovation. This support is welcomed by authors with gratitude. V.P. is grateful to Lithuanian colleagues, R. Miskinis, S. Ragaisis and A. Mitasiunas for the discussions and to R. Hammond of Resonant Inc. for showing interest in the sensor research area. Many thanks to S. Yandrapalli, P. Turner and to J. Koskela for reading the text.

REFERENCES

[1] M. Lamothe, V. Plessky, J.-M. Friedt, T. Ostertag, and S. Ballandras, "Ultra-wideband SAW sensors and tags," Electronics Letters, Volume 49, pp. 1576 – 1577, Issue 24, 21 November 2013, doi:10.1049/el.2013.3333.

[2] D. Morgan, "Surfave acoustic wave filters", Amsterdam, Elsevier, 2007.

[3] S. Harma, V. Plessky, Xianyi Li, and P. Hartogh, "Feasibility of ultra-wideband SAW RFID tags meeting FCC rules", IEEE Transactions on Ultrasonics, Ferroelectrics, and Frequency Control, vol. 56, no. 4, pp. 812-820, April 2009, doi: 10.1109/TUFFC.2009.1104.

[4] D. C. Malocha, D. Puccio, and D. Gallagher, "Orthogonal frequency coding for SAW device applications," IEEE Ultrasonics Symposium, 2004, pp. 1082-1085 Vol.2. doi: 10.1109/ULTSYM.2004.1417965.

[5] V. Plessky and M. Lamothe, "Hyperbolically frequency modulated transducer in SAW sensors and tags", Electronics Letters, Volume 49, Issue 24, p. 1503 – 1504, 21 November 2013, doi: 10.1049/el.2013.2815.

[6] T. Ostertag, RSSI GmbH - Contact. Retrieved January, 2018, from http://www.rssi-gmbh.de/kontakt.html

[7] UWB_SENS | EUROSTARS. Retrieved January, 2018, from https://www.eurostars-eureka.eu/project/id/10640

 ISBN: 978-1-61208-621-7